Fossil organic matter characteristics in permafrost deposits of the northeast Siberian Arctic

Lutz Schirrmeister,[1] Guido Grosse,[2] Sebastian Wetterich,[1] Pier Paul Overduin,[1] Jens Strauss,[1] Edward A. G. Schuur,[3] and Hans-Wolfgang Hubberten[1]

Received 7 January 2011; revised 15 May 2011; accepted 1 June 2011; published 13 September 2011.

[1] Permafrost deposits constitute a large organic carbon pool highly vulnerable to degradation and potential carbon release due to global warming. Permafrost sections along coastal and river bank exposures in NE Siberia were studied for organic matter (OM) characteristics and ice content. OM stored in Quaternary permafrost grew, accumulated, froze, partly decomposed, and refroze under different periglacial environments, reflected in specific biogeochemical and cryolithological features. OM in permafrost is represented by twigs, leaves, peat, grass roots, and plant detritus. The vertical distribution of total organic carbon (TOC) in exposures varies from 0.1 wt % of the dry sediment in fluvial deposits to 45 wt % in Holocene peats. Variations in OM parameters are related to changes in vegetation, bioproductivity, pedogenic processes, decomposition, and sedimentation rates during past climate variations. High TOC, high C/N, and low δ^{13}C reflect less decomposed OM accumulated under wet, anaerobic soil conditions characteristic of interglacial and interstadial periods. Glacial and stadial periods are characterized by less variable, low TOC, low C/N, and high δ^{13}C values indicating stable environments with reduced bioproductivity and stronger OM decomposition under dryer, aerobic soil conditions. Based on TOC data and updated information on bulk densities, we estimate average organic carbon inventories for ten different stratigraphic units in northeast Siberia, ranging from 7.2 kg C m^{-3} for Early Weichselian fluvial deposits, to 33.2 kg C m^{-3} for Middle Weichselian Ice Complex deposits, to 74.7 kg C m^{-3} for Holocene peaty deposits. The resulting landscape average is likely about 25% lower than previously published permafrost carbon inventories.

Citation: Schirrmeister, L., G. Grosse, S. Wetterich, P. P. Overduin, J. Strauss, E. A. G. Schuur, and H.-W. Hubberten (2011), Fossil organic matter characteristics in permafrost deposits of the northeast Siberian Arctic, *J. Geophys. Res.*, *116*, G00M02, doi:10.1029/2011JG001647.

1. Introduction

[2] During the late Quaternary, a large pool of organic carbon accumulated in sedimentary deposits and soils in Arctic permafrost regions, thus representing a significant long-term carbon sink. According to recent estimates the soil organic carbon pool in permafrost regions amounts to about 1672 Pg carbon, corresponding to about 50% of the global belowground organic carbon [*Tarnocai et al.*, 2009]. Calculations of organic carbon mass stored in the upper meter of soil in permafrost regions (496 Pg) double previous estimates for that same region, while for the 0 to 300 cm depth they estimate a carbon store of about 1024 Pg [*Tarnocai et al.*, 2009]. The inventory of organic carbon located deeper than 300 cm is based on very few measurements and therefore connected to strong uncertainties that need to be reduced. Based on first-order estimates from *Zimov et al.* [2006a, 2006b] for a large region in northeast Siberia with ice-rich and organic-rich permafrost of the Yedoma Suite, *Tarnocai et al.* [2009] calculate that 407 Pg of carbon are stored here alone in depths below 300 cm. Similar ice- and organic-rich deposits are reported from Alaska [*Péwé*, 1975] and northwest Canada [*Fraser and Burn*, 1997].

[3] The importance of this large, deep, and long-term pool for modern carbon cycle dynamics becomes clear when we consider that even deep permafrost can be vulnerable to thawing due to climate change and resulting landscape disturbances [*Schuur et al.*, 2008; *Jorgenson et al.*, 2010; *Grosse et al.*, 2011], and actually is warming and thawing in many regions for several decades already [*Romanovsky et al.*, 2010]. Shallow and deep carbon in permafrost can be remobilized by a variety of climate change related processes, such as soil warming, active layer deepening, fires, thermo-

[1]Department of Periglacial Research, Alfred Wegener Institute for Polar and Marine Research, Potsdam, Germany.
[2]Geophysical Institute, University of Alaska Fairbanks, Fairbanks, Alaska, USA.
[3]Department of Biology, University of Florida, Gainesville, Florida, USA.

0148-0227/11/2011JG001647

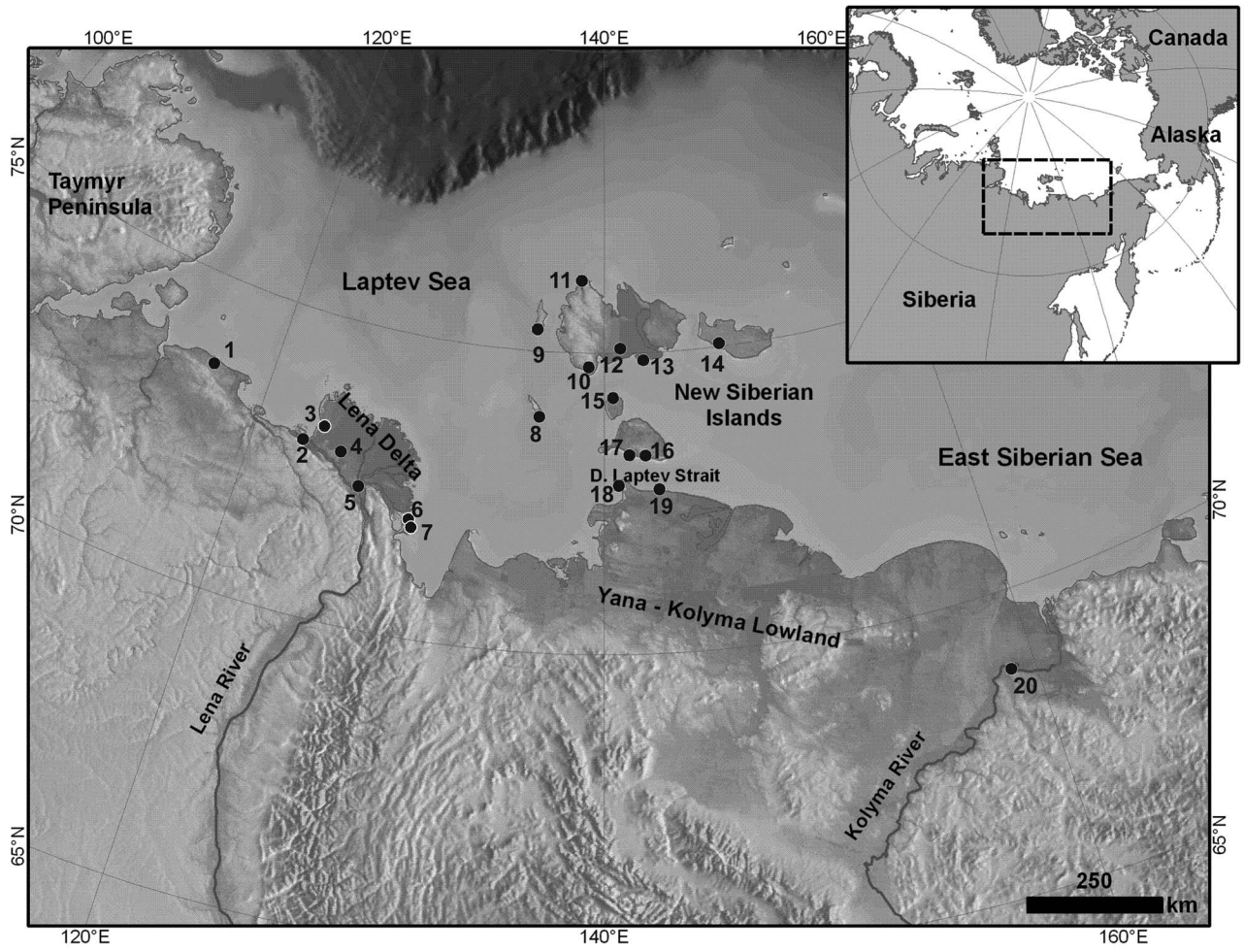

Figure 1. Study sites of permafrost archives in NE Siberia with data sets of fossil organic matter (see also Table 1).

karst, and thermoerosion [*Harden et al.*, 2008; *Grosse et al.*, 2011], allowing microbial turnover of old carbon that was accumulated and stored frozen for long periods of time [*Dutta et al.*, 2006; *Wagner et al.*, 2007]. Various studies indicate that past and future carbon release from permafrost via the greenhouse gases methane and carbon dioxide can cause significant positive feedbacks to climate warming [*Gruber et al.*, 2004; *Walter et al.*, 2007; *Schuur et al.*, 2009].

[4] However, despite strong indications for the significance of the deep permafrost-stored organic carbon pool as a long-term sink in the global carbon cycle, uncertainties in the size and character of this carbon pool remain very high, since only very few field data sets exist [*Tarnocai et al.*, 2009]. Therefore, better knowledge of the distribution of organic matter (OM) in permafrost, its characteristics, and availability for decomposition is required to evaluate current and future carbon dynamics in permafrost regions and their consequences for the global climate system.

[5] Since 1998, northeast Siberian permafrost sequences have been analyzed as frozen archives for Arctic paleoenvironmental and climate dynamics of the last about 200,000 years in the context of the joint Russian-German science cooperation "SYSTEM LAPTEV SEA" [e.g., *Andreev et al.*, 2004, 2009; *Grosse et al.*, 2007; *Schirrmeister et al.*, 2002a, 2002b, 2003, 2008, 2010, 2011a, 2011b; *Wetterich et al.*, 2008, 2009]. In addition to paleoecological, mineralogical and sedimentological data sets, fossil OM data from permafrost deposits have been obtained and interpreted as biogeochemical paleoproxies. Total organic carbon (TOC) values reflect variation in bioproductivity and OM accumulation. The total organic carbon to total nitrogen ratio (TOC/TN, here abbreviated as C/N) indicates the degree of decomposition of OM, initiated by the original vegetation imprint, then modified by microbial activity and pedogenic processes where low C/N values represent stronger decomposed OM and high C/N values represent less decomposed OM [*Carter and Gregorich*, 2008; *White*, 2006]. The content of total inorganic carbon (TIC) mostly depends on the occurrence of freshwater biogenic carbonates (mollusk and ostracod shells) [*Wetterich et al.*, 2005, 2009] but also from source rock detritus. Variations in stable carbon isotope ($\delta^{13}C$) values indicate different origins of OM (e.g., marine, terrestrial, algae, higher land plants) due to different isotopic fractionation during carbon metabolism [*Clark and Fritz*,

Table 1. General Stratigraphic Order for Each Study Site and Relevant Own Publications With Detailed Lithostratigraphic Descriptions[a]

Site ID	Study Site (References)	Lithostratigraphy	Unit[b]
		Western Laptev Sea (1, 2, 3)	
1	Cape Mamontov Klyk	Holocene cover deposits; Holocene valley deposits	h
		Late Glacial to Holocene thermokarst deposits	i
		Late Weichselian Ice Complex	f
		Middle Weichselian alluvial and fluvial deposits	d
		Early Weichselian fluvial deposits	-
		Eemian thermokarst lagoon deposits	-
		Lena Delta (3, 4, 5, 6, 7)	
2	Turakh Sise Island	Holocene deposits	-
		Middle to Late Weichselian fluvial sands	d
3	Ebe Sise Island (Nagym)	Holocene cover deposits	h
4	Khardang Island	Late Glacial to Holocene thermokarst deposits	i
5	Kurungnakh-Sise Island	Late Weichselian Ice Complex	f
		Middle Weichselian Ice Complex	e
		Early Weichselian fluvial deposits	d
		Central Laptev Sea (3, 8, 9)	
6	Bykovsky Peninsula	Holocene cover deposits; Holocene valley deposits	h
7	Muostakh Island	Late Glacial to Holocene thermokarst deposits	i
		Taberite formed during Weichselian to Holocene transition	g
		Late Weichselian Ice Complex	f
		Middle Weichselian Ice Complex	e
		New Siberian Archipelago (3, 10)	
8	Stolbovoy Island	Late Holocene cover deposits	h
9	Bel'kovsky Island	Late Glacial to Holocene thermokarst deposits	i
10	Kotel'ny Island (Cape Anisii)	Middle Weichselian Ice Complex	e
11	Kotel'ny Island (Khomurganakh River)		
12	Bunge Land (low terrace)	Late Holocene alluvial deposits	-
13	Bunge Land (high terrace)	Late Glacial to Holocene thermokarst deposits	i
14	Novaya Sibir Island	Early to Middle Weichselian fluvial deposits	d
15	Maly Lyakhovsky Island	Middle Weichselian Ice Complex	e
		Dmitry Laptev Strait (3, 11, 12, 13)	
16	Bol'shoy Lyakhovsky Island (Vankina river mouth)	Late Holocene cover deposits; Holocene valley deposits	h
		Late Glacial to Holocene thermokarst deposits	i
17	Bol'shoy Lyakhovsky Island (Zimov'e river mouth)	Taberite formed during Weichselian to Holocene transition	g
		Middle Weichselian Ice Complex	e
		Eemian thermokarst lake deposits	c
		Taberite formed during Saalian to Eemian transition	-
		Pre-Eemian flloodplain deposits	b
		Late Saalian ice-rich deposits	a
18	Cape Svyatoy Nos	Middle Weichselian Ice Complex	e
		Pre-Eemian floodplain deposits	b
		Late Saalian ice-rich deposits	a
19	Oyogos Yar coast	Late Holocene cover deposits	h
		Late Glacial to Holocene thermokarst deposits	i
		Taberite formed during Weichselian to Holocene transition	g
		Middle Weichselian Ice Complex	e
		Eemian thermokarst lake deposits	c
		Taberite formed during Saalian to Eemian transition	-
		Kolyma Lowland (14)	
20	Duvanny Yar	Late Holocene cover deposits	h
		Late Glacial to Holocene thermokarst deposits	i
		Middle Weichselian Ice Complex	e
		Eemian thermokarst lake deposits	c

[a]Numbers in parentheses are as follows: 1, *Schirrmeister et al.* [2008]; 2, *Winterfeld et al.* [2011]; 3, *Schirrmeister et al.* [2011b]; 4, *Schirrmeister et al.* [2003]; 5, *Schirrmeister et al.* [2011a]; 6, *Schwamborn et al.* [2002]; 7, *Wetterich et al.* [2008]; 8, *Schirrmeister et al.* [2002a]; 9, *Schirrmeister et al.* [2002b]; 10, *Schirrmeister et al.* [2010]; 11, *Andreev et al.* [2004]; 12, *Andreev et al.* [2009]; 13, *Wetterich et al.* [2009]; 14, *Strauss* [2010] and J. Strauss et al. (Grain-size properties and organic carbon stock of north-east Siberian (Yedoma) Ice Complex deposits, submitted to Global Biogeochemical Cycles, 2011).

[b]Lowercase letters refer to stratigraphic units (see also Figures 2, 3, 5, 6, and 8, Table 2, and Figures S1, S2, and S3) used for the carbon inventory estimation. No samples entered the carbon inventory estimate from lithostratigraphic units marked with a dash.

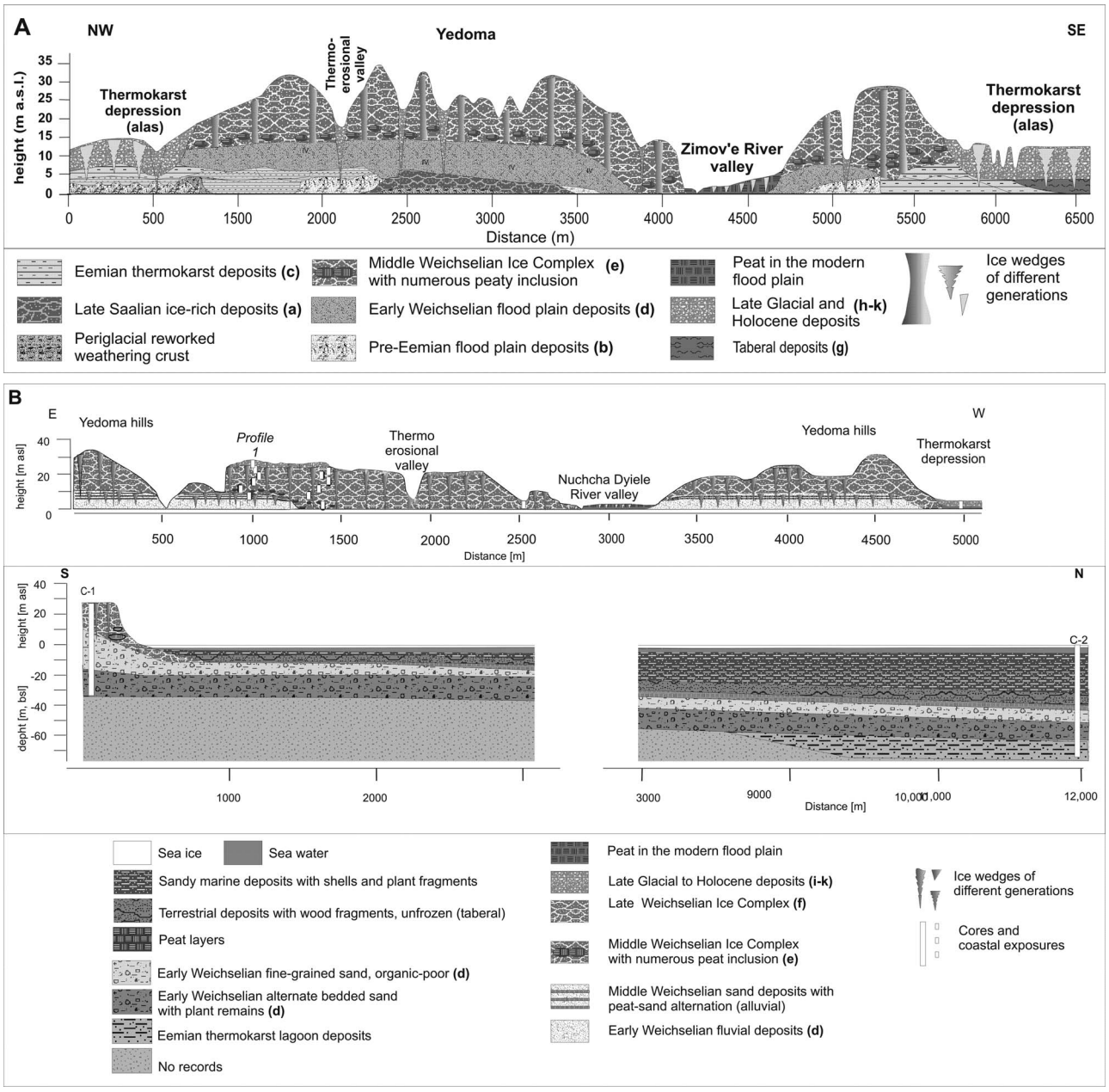

Figure 2. Schematic cross sections of exemplary permafrost sequences. (a) Section exposed at south coast of Bol'shoy Lyakhovsky Island at the Dmitry Laptev Strait (site 17 in Figure 1). (b) Section and drilling transect at Cape Mamontov Klyk in the western Laptev Sea (site 1 in Figure 1).

1997; *Schleser*, 1995; *Meyers*, 2003]. In addition to plant uptake effects, lower $\delta^{13}C$ data corresponds to less decomposed organic matter, while higher $\delta^{13}C$ reflect stronger decomposition [*Gundelwein et al.*, 2007]. Finally, absolute ice contents of frozen ground classified as ice-rich (>50 wt %), ice-bearing (25 to 50 wt %), and ice-poor (<25 wt %) reflect among other factors water availability, soil drainage, temperature, freezing regimes and their dynamics during permafrost formation [*French and Shur*, 2010]. On a global scale, processes of permafrost formation and deformation are strongly controlled by climate variation and the direct and indirect impact on the thermal regime of frozen ground. This is reflected in the variable composition and cryolithological characteristics of permafrost deposits formed and transformed during different late Quaternary climate periods. The relation of ice and OM features in permafrost to climate and lithostratigraphical classifications are essential indicators for understanding past, current and future processes of OM accumulation, preservation, and degradation in permafrost soils.

[6] The major objective of this paper is (1) to summarize new regional data sets on the quality and quantity of fossil OM in late Quaternary permafrost sequences of NE Siberia, (2) to characterize the heterogeneity of carbon pools in per-

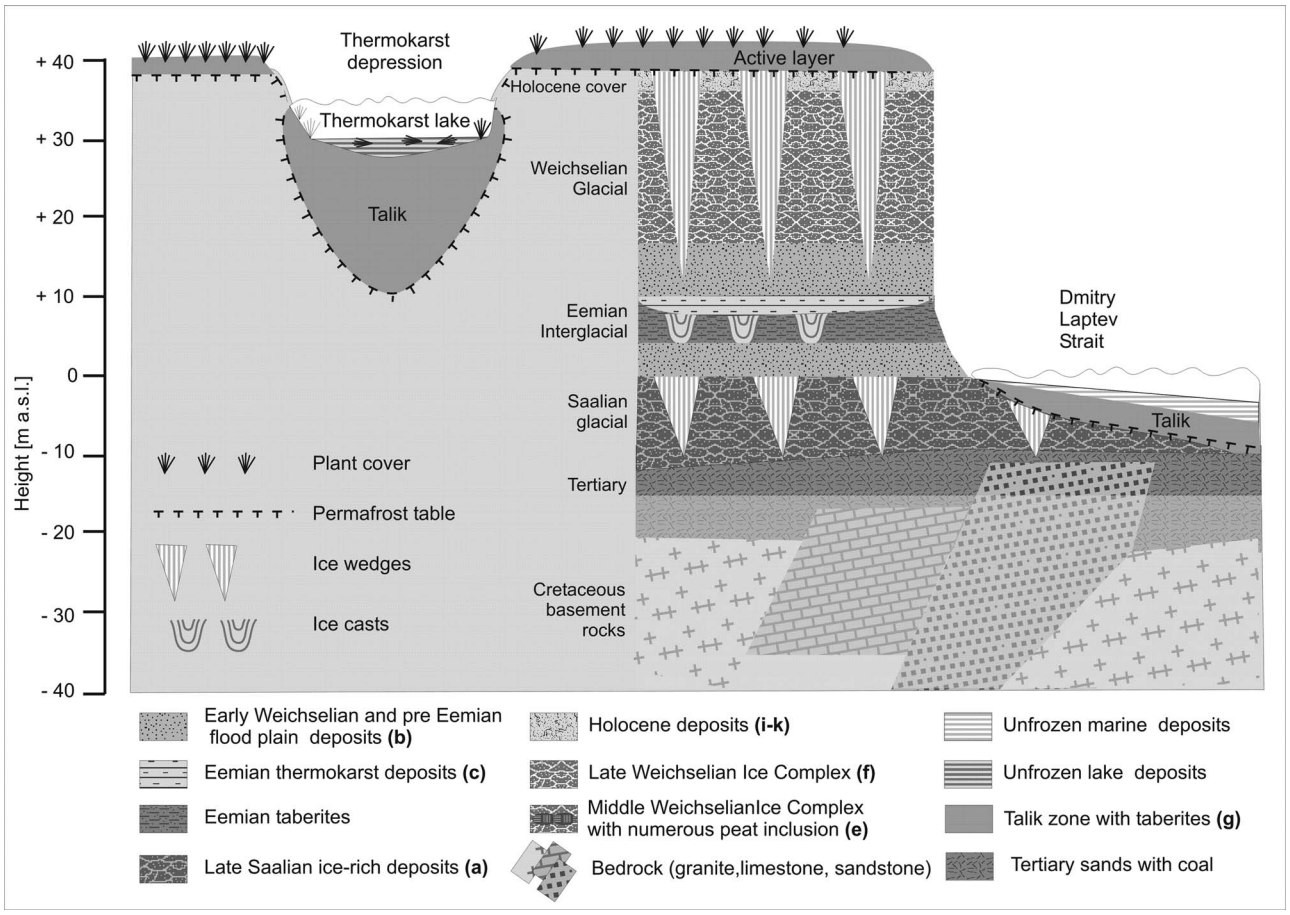

Figure 3. General scheme of the stratigraphical segments of the permafrost zone and several components of arctic periglacial landscapes at the Dmitry Laptev Strait.

mafrost deposits as related to stratigraphy and depositional history, and (3) to improve quantification of permafrost carbon stocks in order to understand the vulnerability of such pools to climate change and disturbances.

2. Study Sites

[7] All studied sites are located in the continuous permafrost region of northern East Siberia. The region is characterized by a broad variety of terrestrial syngenetic and epigenetic permafrost sediments [*Yershov*, 1989, 1991]. A total of twenty exposures on the coasts of the Laptev and East Siberian seas as well as on river banks in the Lena Delta and the Indigirka-Kolyma lowland (Figure 1 and Table 1) were investigated for OM characteristics of the permafrost deposits. The locations were primarily selected to study in detail the stratigraphic and paleoenvironmental significance of late Pleistocene and Holocene frozen terrestrial and aquatic deposits, with a focus on late Pleistocene Ice Complex deposits of the Yedoma Suite [*Schirrmeister et al.*, 2011b; *Zimov et al.*, 2006a, 2006b]. However, according to our cryolithological, paleoecological, and geochronological data sets, the profiles of all twenty sites represent different stratigraphical cross sections and cover a wide range of depositional environments in periglacial landscapes during the late Quaternary (Table 1). Generally, such exposures at sea coasts and river banks are naturally formed by active thermoerosion and slumping of ice-rich permafrost, exposing sediments and ground ice in rapidly retreating steep bluffs and terraces and allowing access to still-frozen sediments in vertical profiles of 3 to 40 m total height.

[8] Typical exposures included Yedoma elevations, which are largely composed of Weichselian Ice Complex deposits, Holocene thermokarst depressions filled with lacustrine and boggy deposits, and sometimes underlying older strata (Figure 2a). In some cases, exposures were extended below current sea level by drilling into terrestrial sediments onshore and offshore on the continental shelf, allowing investigation of permafrost OM characteristics down to more than 100 m depth at some sites (Figure 2b).

[9] A generalized stratigraphical scheme (Figure 3 and Table S1) includes several typical main depositional components of the upper permafrost zone in the study region: Tertiary sands with coal inclusions; late Saalian (200 to 150 ka) ice-rich deposits (Ice Complex); pre-Eemian (>130 ka) alluvial (floodplain) deposits; Eemian (130 to 110 ka) thermokarst lake and lagoon deposits; early Weichselian (100–60 ka) fluvial and alluvial (floodplain) deposits; middle and late Weichselian (60 to 15 ka) ice-rich deposits (Ice Complex, Yedoma Suite); late glacial (15 to 10 ka) and early Holocene (10 to 8 ka) basin deposits

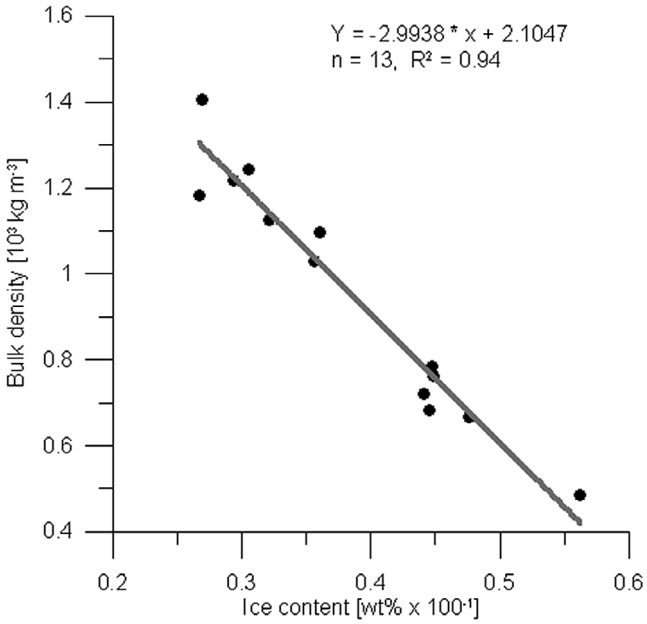

Figure 4. Relationship between absolute ice content and bulk density of Ice Complex samples collected at multiple sites in the Kolyma River region.

including lacustrine sediments and terrestrial peat; and Holocene (10 ka to modern) cover deposits.[1]

3. Methods

[10] Complete exposure profiles in a particular area were sampled in numerous overlapping subprofiles of 1 to 5 m height across the bluffs depending on access to frozen sediments, which then were merged into a representation of the site-specific stratigraphy of the permafrost deposit. Field investigations in the outcrop exposures included cryolithological characterization, lithostratigraphical differentiation, and collection of several hundred samples to be analyzed for lithology, OM and ground ice characteristics. About 0.5 to 1.0 kg of frozen autochthonous sediment per sample was taken and stored in plastic bags. The ice content was estimated immediately after thawing in the field by weighing the wet sample, then drying and reweighing to compare the weight loss (water/ice content) to the total weight of the wet sample, expressed as weight percentage (wt %). Upon return to the laboratory the samples were freeze-dried, carefully manually homogenized and split into subsamples for various purposes. The contents of total organic carbon (TOC), total carbon (TC), and total nitrogen (TN) were measured with a CNS analyzer (Elementar Vario EL III). For TOC measurement, samples were pretreated by HCl to remove carbonate, while TC values were estimated without such pretreatment. The C/N ratio was calculated as the quotient of TOC and TN values if TN values were >0.05 wt %. The total inorganic carbon (TIC) values were calculated by the difference between total carbon (TC) and TOC. Stable carbon isotopes (δ^{13}C) of TOC were measured with a Finnigan DELTA S mass spectrometer if TOC values were >0.3 wt %. The δ^{13}C values are expressed in delta per mil notation (δ, ‰) relative to the Vienna Pee Dee Belemnite (VPDB) standard and the analyses were accurate to ±0.2‰. In total, 806 samples were analyzed for ice content, 1281 for TOC, 1062 for TIC, 882 for C/N, and 865 for δ^{13}C, providing a comprehensive data set on fossil organic carbon characteristics for permafrost deposits of northeast Siberia. The organic carbon inventory was calculated by converting ice content measurements (wt %) into bulk density (10^3 kg m^{-3}) using a linear relationship (R^2 = 0.94; $p < 0.01$; Figure 4) developed for a subset of thirteen Ice Complex samples collected at multiple sites in the Kolyma River region [*Dutta et al.*, 2006. In soil science, the bulk density is a standard parameter describing the dry mass of a volume unit of soil that accounts for both the density of the solid materials as well as the pore volume [*Scheffer and Schachtschabel*, 2002]. In ice-rich permafrost deposits, the pore volume is entirely filled by ice and the ice content is considered an equivalent of the pore volume. Excess ice content can increase the pore volume to higher values than possible for unfrozen water saturated sediments, and thus is a strong control of overall bulk density. The organic carbon inventory of the frozen sediment (kg C m^{-3}) was bulk density multiplied by percent organic carbon. Frequent massive ice wedges which, according to numerous own field observations and compilations by other workers [e.g., *Romanovskii*, 1977; *Zimov et al.*, 2006a, 2006b; *Kanevskiy et al.*, 2011], can be 50 to 80% of the permafrost volume and are not included in this calculation.

4. Results

4.1. Organic Matter Components and Their Origin

[11] The late Quaternary permafrost deposits contained OM largely originating from fossil plant detritus, mosses, rootlets, seeds, leafs, filamentous grass roots, woody fragments of shrub roots and twigs, and single stems of small trees. Plant OM is often accumulated in buried cryosols, in peaty layers, in individual peaty inclusions, and in plant detritus layers of lacustrine origin. However, fine dispersed OM detritus embedded within a mineral soil matrix is also common. More detailed data on the composition of plant OM are available from palynological and carpological studies of past vegetation dynamics in the study region [e.g., *Anderson and Lozhkin*, 2001; *Andreev et al.*, 2011; *Giterman et al.*, 1982; *Kaplina*, 1981; *Kienast et al.*, 2005, 2008, 2011; *Wetterich et al.*, 2008, 2009]. In addition, some OM originates from fossil faunal remains that are found in permafrost deposits, including large and small mammal bones, insects, and aquatic organisms. Fossil soil microorganisms, fungi, algae, and lichen also add to the permafrost OM.

[12] Several cryolithological facies types typical of periglacial lowlands were distinguished within the studied permafrost sections and cores. Deposits with very high excess ice content, large syngenetic ice wedges, and lens-like reticulated cryostructures are termed Ice Complexes (in Russian: ledovyi complex, according to *Soloviev* [1959]). Their OM content is characterized by cryosols, peat inclusions, and fine-distributed plant detritus that accumulated in a polygonal tundra or tundra-steppe landscape. In the study region, an ice-rich deposit similar to the Yedoma Ice

[1] Auxiliary materials are available in the HTML. doi:10.1029/2011JG001647.

Complex already accumulated during a late Saalian stadial and a following interstadial period (Figures 2a and 3). Sparse grass-/sedge-dominated vegetation was the major organic carbon source for soils and sediments during late Saalian stadial times, but dense grass-dominated tundra followed under more temperate interstadial climate conditions [*Andreev et al.*, 2011]. Syngenetic permafrost development and cryoturbation resulted in rapid burial of OM into permafrost. Cryoturbation occurs in varying degrees in most of the paleosols in this and all overlying strata. During the Pre-Eemian stadial the presence of green algae spores in sediments is indicative of the occurrence of polygonal ponds in otherwise a sparsely vegetated grass/sedge tundra. Large amounts of plant OM were found in Eemian thermokarst deposits preserved in ice wedge casts (where ice wedges had melted during previous warm periods) and in lacustrine sediments. The Eemian vegetation was mainly composed of grass/sedge associations, with some herbs, birch, alder, and willow shrubs, and larch, birch and alder trees presenting an open shrub tundra to forest tundra. In addition, wetland, riparian and aquatic plants were present, reflecting lacustrine thermokarst conditions [*Andreev et al.*, 2011; *Kienast et al.*, 2008, 2011; *Wetterich et al.*, 2009].

[13] Loess-like floodplain deposits accumulated during late Saalian and early Weichselian cold periods containing remains of sparse grass/sedge vegetation, preserved as filamentous grass roots. In the early Weichselian, fluvial sands accumulated in many regions of the study area but very little plant OM was found in these deposits, including dispersed plant detritus mixed with mineral soil or peat layers that accumulated under stagnant water conditions in abandoned river channels and oxbow lakes. In general, the early Weichselian was also dominated by sparse tundra-steppe vegetation, forming the major source of OM in permafrost deposits during this stadial period.

[14] Alluvial deposits on top of fluvial sands accumulated in polygonal ice wedge systems on floodplain terraces under less severe middle Weichselian interstadial climate conditions, resulting in accumulation of large amounts of OM, in particular moss peat. During this period, Ice Complex deposits of the Yedoma Suite were formed in a polygonal landscape, which was characterized by patchwork-like distribution of a variety of vegetation communities. A dense, herb-dominated grass-sedge vegetation with few shrubs [*Andreev et al.*, 2011; *Kienast et al.*, 2005], previously termed the "*tundra-steppe*" [*Yurtsev*, 2001], produced large amounts of plant organic matter in permafrost. The OM of the middle Weichselian is largely composed of peat inclusions, peat lenses, woody twig and root fragments, filamentous grass roots, and disperse plant detritus mixed with mineral soil. In addition, Yedoma Ice Complex sequences contain aquatic floral and faunal elements like algae and zooplankton, and large amounts of mammal bones of the mammoth fauna [*Sher et al.*, 2005]. Late Weichselian stadial parts of Ice Complex deposits contain less plant OM represented by sparse tundra-steppe vegetation as compared to the middle Weichselian [*Andreev et al.*, 2011].

[15] Large amounts of organic matter in permafrost regions were reworked and deposited in thermokarst depressions formed as permafrost thawed and the ground subsided due to loss of ground ice volume during the late glacial to early Holocene transition. Such depressions are a dominant landform of the modern relief of NE Siberian Arctic lowlands. Deposits in thermokarst depressions are often composed of lacustrine sediments that accumulated in thermokarst lakes beginning already in the late glacial interstadial periods. These thermokarst lake sediments contain OM resulting from reworking and deposition of older material eroded from shore bluffs into the lake by thermal erosion typical for thermokarst lakes in addition to in situ production of new OM from aquatic plants and animals.

[16] Lacustrine sediments are often followed by Holocene peat bog deposits that accumulated in ice wedge polygonal systems after lake basins had drained, which is typical process during the evolution of permafrost landscapes [*Wetterich et al.*, 2009]. The late glacial vegetation is generally described as grass-/sedge-dominated vegetation with willow and birch shrubs [*Andreev et al.*, 2011]. Aquatic plants and algae occurred as well as faunal associations of ostracods and mollusks [*Wetterich et al.*, 2005, 2008, 2009].

[17] Besides the syncryogenic and epicryogenic deposits frozen during or after their accumulation described above, so-called taberite deposits (frozen sediments thawed under thermokarst lakes and then refrozen after lake drainage) are connected with former taliks (thaw bulbs) below thermokarst lakes of the Eemian and late glacial to early Holocene periods. Such transformed deposits are characterized by a dense appearance caused by low ice content and coarse lattice-like ice structures. Plant remains are only seldom visible. Taberites contain more strongly decomposed plant OM than unaltered Ice Complex deposits, reflecting partial decomposition of OM in thawed zones under lakes [*Wetterich et al.*, 2009].

4.2. Organic Matter Heterogeneity in Vertical Permafrost Profiles

[18] Considering the site-specific characteristics of permafrost deposits as determined with cryolithological, geochronological, and paleoecological methods, stratigraphical units are often characterized by specific carbon and OM features, which additionally can vary within single units. The important stratigraphic units used to estimate the C inventory are labeled with small letters (a to k) in Tables 1 and 2; Figures 2a, 2b, 3, 5, 6, and 8; and Figures S1, S2, and S3. Two key sites (Figures 5 and 6) are presented in this section to highlight the spatial and temporal variability of OM parameters in late Quaternary permafrost. Data sets from three more key sites from the Lena Delta, the Bykovsky Peninsula and the Duvanny Yar section (sites 2–5, 6, 7, 20 in Figure 1) are available in the auxiliary material (Figures S1, S2, and S3).

[19] A comprehensive permafrost record representing the last ~200,000 years is available from the south coast of Bol'shoy Lyakhovsky Island at the coast of the Dmitry Laptev Strait (sites 16, 17 in Figure 1) [*Schirrmeister et al.*, 2002b; *Andreev et al.*, 2004, 2009; *Wetterich et al.*, 2009]. Numerous subprofiles were studied from sea level at the beach up to about 30 m above sea level (asl) (Figure 2a). Figure 5 combines records of selected key profiles of site 17 (Figure 1) in stratigraphical order from a ~20 km long coastal segment. The oldest horizon, classified as late Saalian ice-rich deposits (unit a), is characterized by ground ice contents of frozen sediments of 20 to 80 wt %, massive syngenetic ice wedges of several meters width, TOC con-

Table 2. Carbon Inventory Estimates for Different Stratigraphical Units According to Average and Range Data Across All Sites in Figure 8 and Table S2[a]

Unit	Stratigraphical Units	Ice Content (wt %)	Estimated Bulk Density (10^3 kg m^{-3})	TOC (wt %)	Carbon Inventory (kg C m^{-3})	SD[b]
k	Holocene thermoerosional valley	44.2 ± 9.0	0.781	5.3 ± 4.9	41.42	40.87
i	Holocene thermokarst	44.4 ± 16.0	0.775	6.9 ± 9.0	53.51	77.22
h	Holocene cover	47.4 ± 14.5	0.686	10.9 ± 12.9	74.73	96.26
g	Taberites	28.8 ± 4.8	1.242	2.7 ± 1.4	33.55	17.82
f	Late Weichselian Ice Complex	38.3 ± 12.5	0.958	2.2 ± 0.9	21.08	11.92
e	Middle Weichselian Ice Complex	40.5 ± 12.8	0.892	3.7 ± 4.1	33.23	40.07
d	Early to Middle Weichselian fluvial deposits	22.4 ± 11.3	1.434	0.5 ± 1.4	7.17	18.72
c	Eemian lake deposits	29 ± 8.3	1.236	3.2 ± 4.2	39.57	50.10
b	Pre-Eemian floodplain	32.6 ± 8.3	1.129	1.0 ± 0.8	11.29	8.28
a	Saalian ice-rich deposits	58.7 ± 20.1	0.347	5.3 ± 4.3	18.41	34.93

[a]Note that these estimates are for frozen sediment and soil and do not account for presence of ice wedges.
[b]Propagated error.

tents varying between 2.8 and 12.7 wt %, C/N ratios of 5.3 to 24.1, and δ^{13}C values between −28.7 and −26.8‰. The following Pre-Eemian floodplain deposits (unit b) show a completely different patterns with low ice contents (20 to 30 wt %), very thin epigenetic ice wedges, and low TOC contents (~0.5 wt %). C/N ratios (0.7 to 6.7) are rather low, and δ^{13}C values are higher (−25.3 to −24.9‰) as compared to the underlying sediments of unit a. Eemian thermokarst lake deposits (unit c) exposed in ice wedge casts contain only little ground ice (20 to 30 wt %) and have variable TOC (0.7 to 5.1 wt %). Single layers with strikingly high TIC contents of up to 7 wt % mark the occurrence of mollusks and ostracod shells. Peaty layers (not shown in Figure 5) covering the Eemian ice wedge cast horizon are characterized by high ice contents (54 to 75 wt %), high TOC contents (up to 17 wt %), a relative even C/N ratio (10 to 14), and very low δ^{13}C values of −30.6 to −28.9‰.

[20] The overlying middle Weichselian Ice Complex sequence (unit e) is about 15 m thick and characterized by 30 to 62 wt % ice content, large syngenetic ice wedges, and TOC contents of 1 to 4 wt % except of a peaty cryosol horizon containing 5 to 17 wt % TOC. C/N ratios are strongly varying between 1 and 20 especially in the lower segment with higher TOC contents, whereas the upper part is marked by more consistent C/N ratios of about 10. The δ^{13}C values (−26.1 to −24.5‰) are rather high and consistent, except of the peaty cryosol horizon characterized by low δ^{13}C values (−29.1 to −27‰). The carbon isotope signature of thawed and refrozen Ice Complex material of taberite (unit g) exposed below thermokarst deposits is different from Weichselian Ice Complex deposits with the lowest δ^{13}C values at −31 to −30‰.

[21] Finally, late glacial to early Holocene lacustrine sediments deposited in a thermokarst depression (unit i) contained 20 to 30 wt % ice and 1.5 to 3.7 wt % TOC. The C/N ratio was low and uniform (3 to 8) and the δ^{13}C values varied between −28.8 and −26.5‰. The uppermost peat cover in the thermokarst depression was clearly distinguished from the underlying lacustrine sequence by high TOC contents (8 to 13.6 wt %), C/N rations of 13 to 15 and very low δ^{13}C values of −30.9 to −30.3‰.

[22] At the second key site at Cape Mamontov Klyk in the western Laptev Sea (site 1 in Figure 1), permafrost deposits were studied at coastal cliffs up to 30 m asl while an additional 70 m deep core was drilled below sea level (bsl). Hence, the studied permafrost sequence (Figure 2b) covers the upper 100 m of permafrost at this site [*Winterfeld et al.*, 2011]. Available OM characteristics are combined and summarized in Figure 6. The lowermost horizon of probably Eemian thermokarst lagoon deposits is characterized by low TOC contents (0.2 to 1.2 wt %), low TIC contents (0.1 to 0.3 wt %), an even C/N ratio between 9 and 12, and rather high δ^{13}C values (−26.9 to −24.8‰). These deposits form a cryopeg, i.e., an unfrozen but perennially cryotic zone in permafrost because of freezing point depression due to high salinity of the pore water. According to the bedded sediment structure of the overlying early Weichselian fluvial deposits (unit d) and the occurrence of layers with plant detritus and woody fragments, the OM parameters are strongly varying in the overlying horizon. A several decameter thick sequence of fluvial and lacustrine fine-grained sand that also belong to unit d contained little organic matter. Therefore, C/N and δ^{13}C values were determined from single plant detritus layers. Middle Weichselian alluvial peat-sand alternations covering the underlying sands of unit d are characterized by high ice contents (up to 70 wt %), varying TOC contents (between 0.2 and 15.3 wt %), and correspondingly variable C/N (between 2 and 25) and δ^{13}C values (−27.7 to −23.2‰).

[23] Late Weichselian Ice Complex deposits (unit f) contain 35 to 70 wt % of excess ice, large syngenetic ice wedges, and depending on the presence or absence of cryosol horizons 1.4 to 8.5 wt % TOC. Higher TIC contents of 1 to 2.2 wt % are related to the occurrence of mollusk and ostracod shells. Holocene deposits of a thermokarst depression unit (i) and a thermoerosional valley (unit k) composed of peaty cryosols are characterized by similar excess ice contents between 25.8 and 62.2 wt % and, except for the uppermost peat cover (unit h) by rather uniform values of OM parameters. The peat cover is characterized by high ice contents (46 to 74 wt %), high TOC values (4 to 22 wt %), low δ^{13}C (about −28‰), and high C/N ratios (14.5 to 16).

[24] The organic C inventory within the frozen sediment component of the ten major stratigraphical units (a to k) varied by more than a factor of 10 from about ~7 kg C m^{-3} in the Early Weichselian fluvial deposits (unit d) to more than 70 kg C m^{-3} in the Holocene cover unit (unit h) (Table 2). On average, Yedoma Suite Ice Complex units contain about 21 to 33 kg C m^{-3} across all sampled profiles (Table 2). Between the selected Yedoma sites shown in Figure 7, the organic C inventories range between 14 kg C m^{-3} at Duvanny

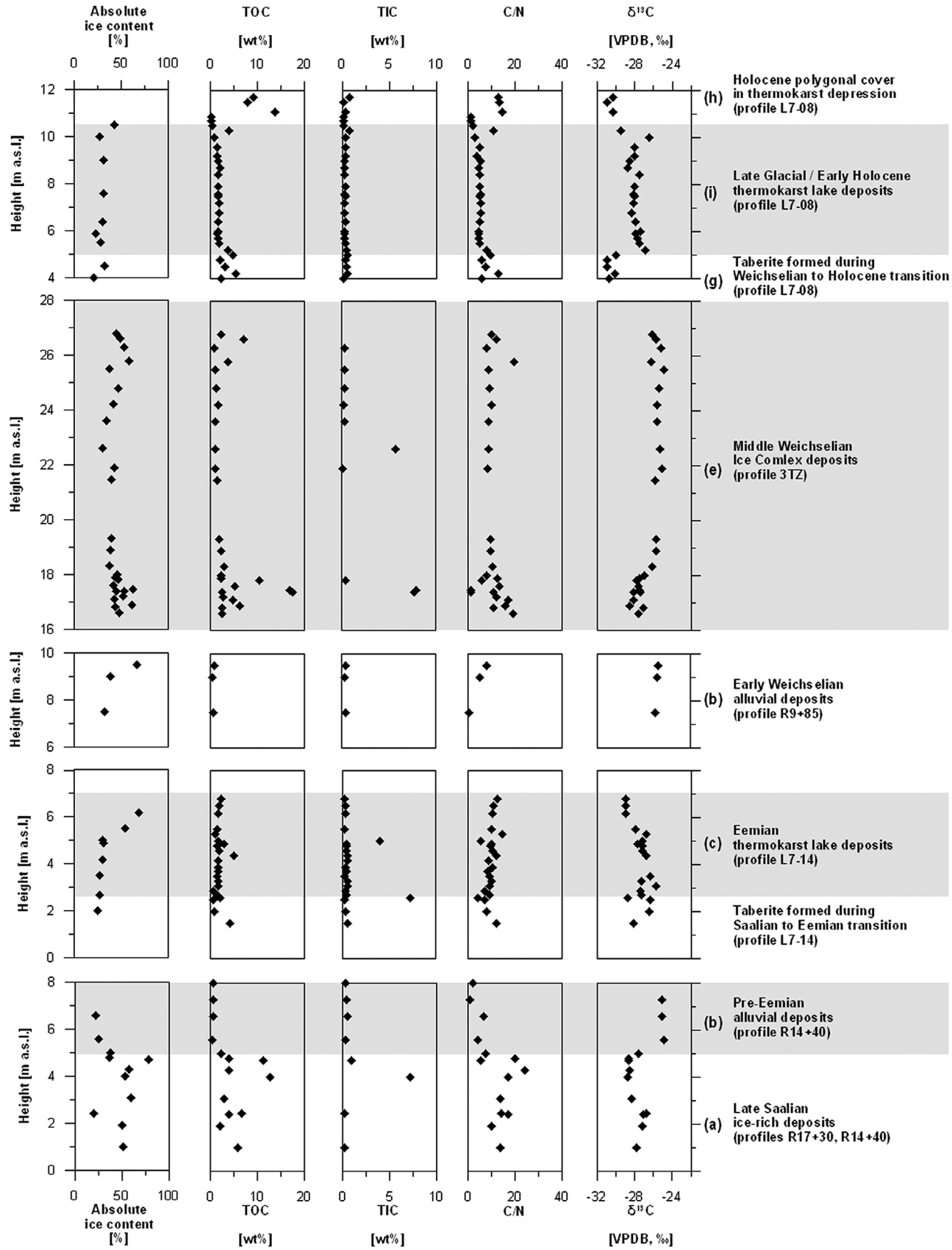

Figure 5. Exemplary compilation of ice content and OM signatures of permafrost sequences at the Dmitry Laptev Strait (site 17 in Figure 1; Bol'shoy Lyakhovsky) described by *Wetterich et al.* [2009], *Schirrmeister et al.* [2011b], and *Andreev et al.* [2009, 2004].

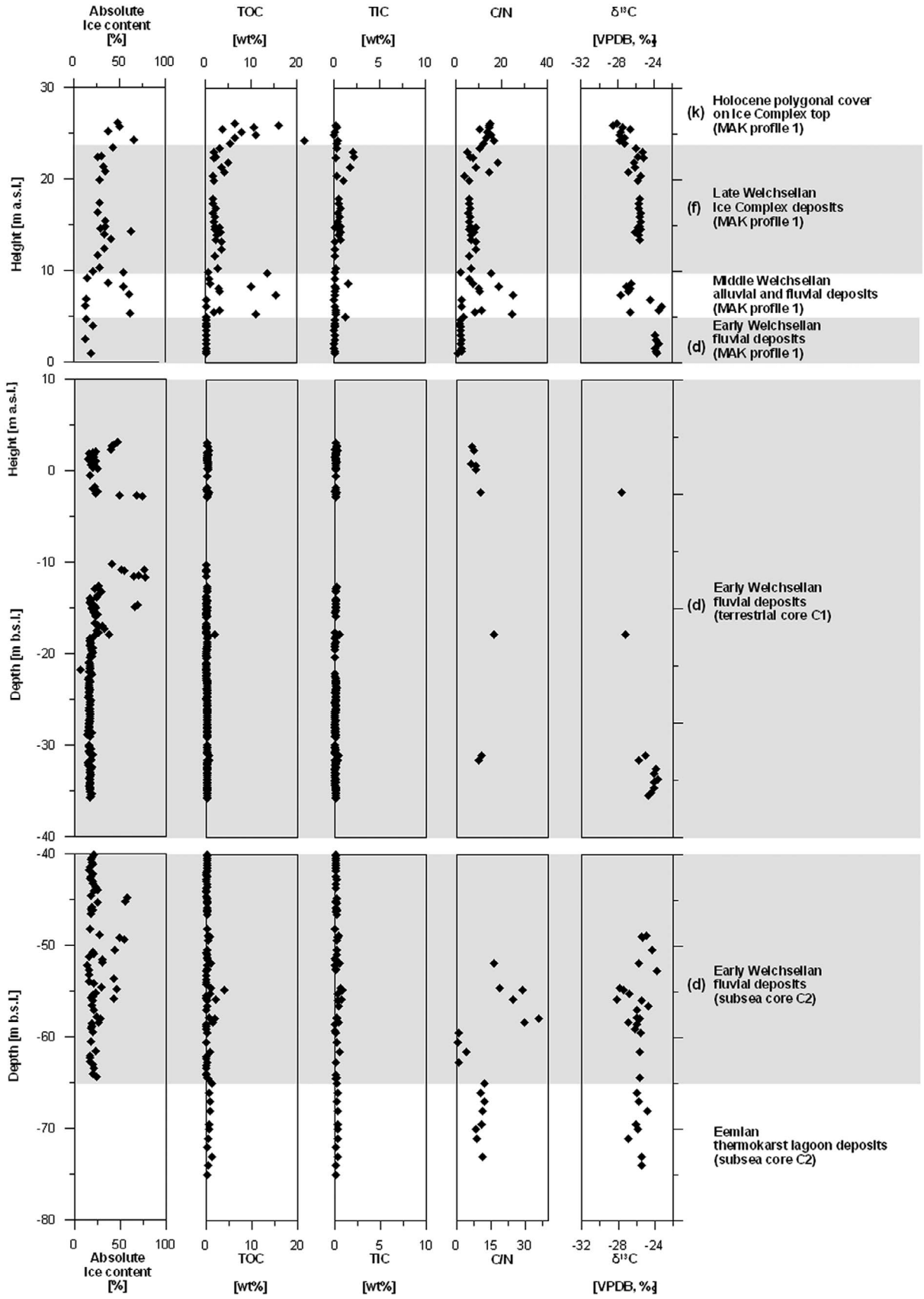

Figure 6. Exemplary compilation of ice content, carbon, and OM signatures of permafrost sequences in the western Laptev Sea coastal area (site 1 in Figure 1; Cape Mamontov Klyk) described by *Schirrmeister et al.* [2008] and *Winterfeld et al.* [2011].

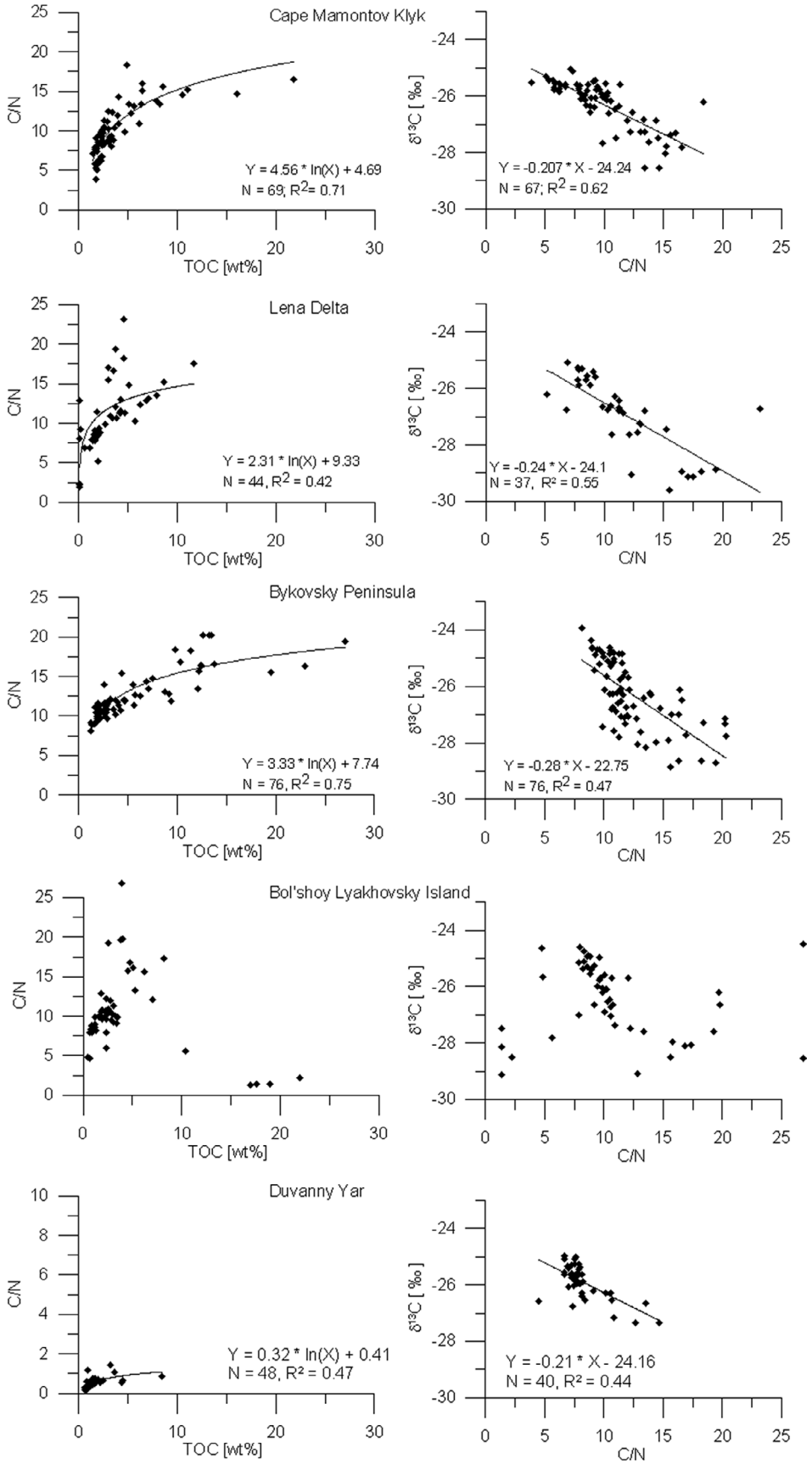

Figure 7. Correlation of OM signatures (TOC, C/N, $\delta^{13}C$) of Yedoma Ice Complex deposits from different key sites (sites 1, 5, 6, 17, and 20 in Figure 1 and Table 1).

Table 3. Estimated Soil Carbon Inventory of Yedoma Ice Complex Deposits for the Individual Five Sites Mentioned Exemplarily in the Text[a]

Site Number in Figure 1 and Table 1	Individual Sites	Total C Content (kg C m^{-2})	Total Depth (m)	Average Carbon Inventory Across Measured Profile (kg C m^{-3})	SD
1	Cape Mamontov Klyk	315.44	12.70	24.84	14.17
5	Lena Delta	553.33	18.25	30.32	16.13
6	Bykovsky Peninsula	910.20	36.35	25.04	13.41
17	Bol'shoy Lyakhovsky Island	180.75	10.20	17.72	20.08
20	Duvanny Yar	596.46	42.00	14.20	7.90

[a]This does not account for the presence of ice wedges volume.

Yar and 30 kg C m^{-3} in the Lena Delta (Table 3). At individual sites, organic C inventories in the Yedoma Ice Complex vary strongly with a standard deviation of 8 to 20 kg C m^{-3} (Table 3). These amounts take into consideration the ice and organic C content of the frozen soil, but do not account for the presence of ice wedges, which further reduces the organic C inventory at the landscape scale.

5. Discussion

[25] According to our comprehensive data set of OM characteristics, the TOC and TIC contents, the OM composition, and the decomposition degree are highly variable between and sometimes also within individual stratigraphical units. The OM signatures of late Quaternary permafrost deposits reflect different local landscape and sediment facies conditions in the accumulation area that affected factors important for OM preservation and incorporation into permafrost: hydrology and soil moisture regime; vegetation cover, organic surface litter production and decomposition; soil formation, cryoturbation and sedimentation rates; subsurface microbial decomposition; freezing and thawing conditions in the active layer; and aggradation of permafrost [*Grosse et al.*, 2011].

[26] Specific sediment accumulation conditions at the studied sites include alluvial, fluvial, limnic, proluvial and aeolian processes. For all studied sites we found that remains of terrestrial C3 plants dominate the composition of OM, which is evident by $\delta^{13}C$ values between −31.4 and −23.4‰. Generally, the OM characteristics in permafrost deposits differ between horizons accumulated during temperate interglacial or interstadial periods, and those accumulated during harsh glacial or stadial periods (Figure 8). The OM character between various units is therefore largely controlled by changes in paleoclimatic conditions during late Quaternary climate cycles and related paleoenvironmental dynamics, in particular those of landscape and veg-

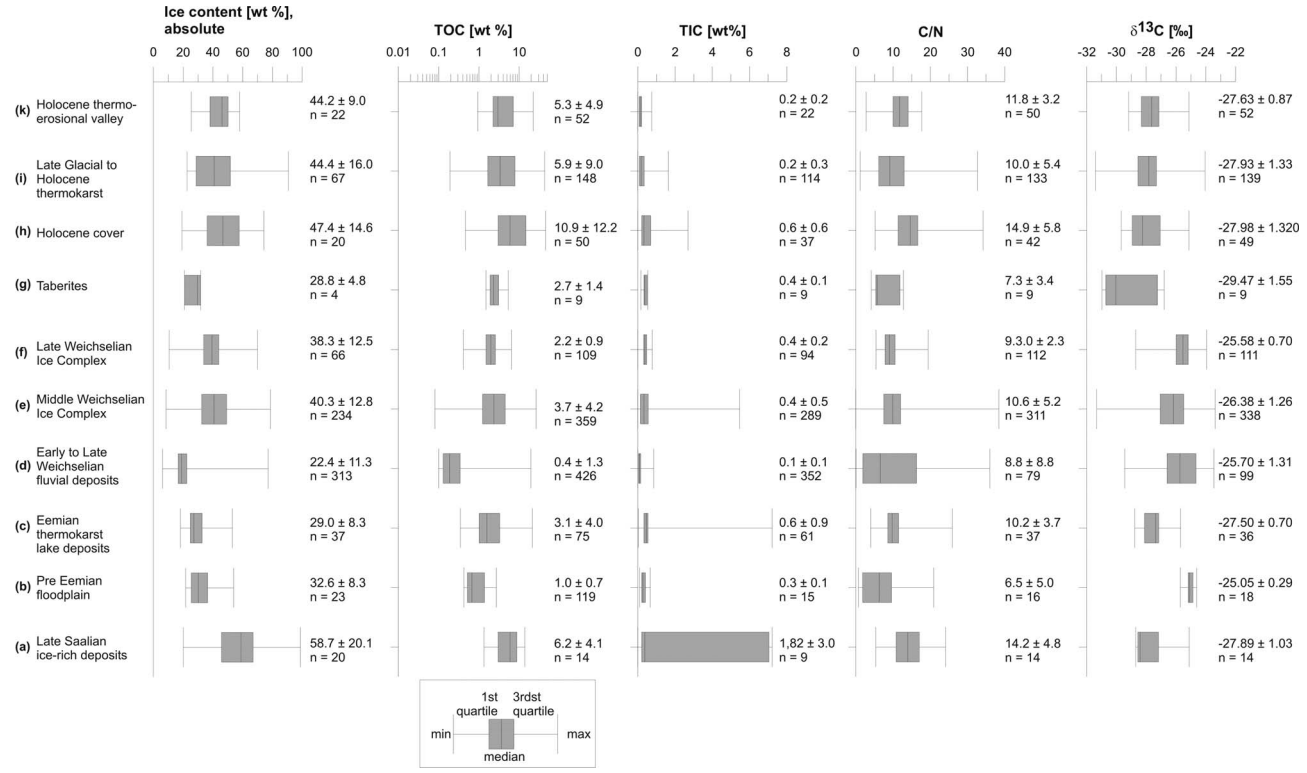

Figure 8. Stratigraphical classification of permafrost deposits by OM signatures and ice content. Note the logarithmic scale for the TOC values.

etation. For example, syngenetic permafrost formation with ice wedge growth in polygonal tundra landscapes over long interstadial periods in the late Pleistocene led to rather intense accumulation and frozen preservation of plant remains, which today is illustrated by less decomposed OM and high TOC. On the contrary, fluvial-dominated accumulation during the same time period but at other locations led to rather low OM contents. Deposits formed during interglacial thermokarst formation, identified both for the Eemian and the Holocene, still store considerable amounts of reworked OM. High carbon inventories in thermokarst lake deposits are partially related to a concentration effect for reworked OM as thaw subsidence progresses. Therefore, thermokarst lakes and basins can act as a local sink for portions of the carbon released from thawing permafrost deposits, while at the same time thermokarst lakes also result in intense OM degradation and methane production in the anaerobic environments of organic-rich lake sediments and taliks [*Walter et al.*, 2006]. Post-lake drainage peat growth sequesters carbon from the atmosphere and increases the carbon inventory of thermokarst depressions, while at the same time these polygonal peatlands are methane emitters (M. Jones et al., Peat accumulation in a thermokarst-affected landscape in continuous ice-rich permafrost, Seward Peninsula, Alaska, submitted to *Journal of Geophysical Research*, 2011).

[27] In order to illustrate the relationship between OM parameters, in particular between TOC and C/N ratio, and between C/N ratio and $\delta^{13}C$, we plotted diagrams for Weichselian Yedoma Ice Complex deposits from various locations (Figure 7). There is a logarithmic correlation between TOC contents and C/N ratios that fits best for the Ice Complex deposits at Cape Mamontov Klyk and on Bykovsky Peninsula (Figure 7; $R^2 = 0.71$ and $R^2 = 0.75$, respectively). Except for the Ice Complex on Bol'shoy Lyakhovsky a similar pattern was observed for other sites. Maximum C/N ratios of about 25 were also paired with maximum values of TOC with up to 30 wt %. A rather linear correlation between C/N and $\delta^{13}C$ values, indicating the degree of OM decomposition, was be found best expressed in the Ice Complex deposits at Cape Mamontov Klyk (Figure 7; $R^2 = 0.62$) and similarly for other sites.

[28] As the plant remains in Weichselian Yedoma Ice Complex deposits all represent similar grass/sedge tundra vegetation, variation in TOC content, C/N ratio, and $\delta^{13}C$ values are connected to changes in the bioproductivity, intensity and character of cryosol formation, and different degrees of OM decomposition under subaerial or subaquatic conditions. Variations in plant associations depending on general climate changes are also obvious and lead to changes in OM characteristics [*Andreev et al.*, 2011; *Guthrie*, 1990; *Kaplina*, 1981; *Kienast et al.*, 2005, 2008, 2011; *Wetterich et al.*, 2008, 2009; *Yurtsev*, 2001]. High TOC contents, high C/N ratios, and low $\delta^{13}C$ values reflect less decomposed organic matter under anaerobic conditions [*Gundelwein et al.*, 2007] which are characteristic for the middle Weichselian interstadial when intense soil formation and peat accumulation in a polygon tundra landscape took place. Stadial or glacial periods are characterized by less variable, generally low TOC contents with low C/N ratios, which indicate stable environments with reduced bioproductivity and higher decay rates. High $\delta^{13}C$ values also reflect these relatively dry, aerobic conditions.

[29] Carbon dynamics in permafrost regions interact strongly with several components of the Earth's climate system. The release of carbon from permafrost and its transfer to the atmosphere and hydrosphere occurs largely via the active layer [*Wagner et al.*, 2007; *Schuur et al.*, 2009], via thermokarst lakes and their thaw bulbs [*Walter et al.*, 2006], via export of dissolved and particulate carbon with streams [*Frey and McClelland*, 2009], and via erosion of coasts, lake and river shores [*Jorgenson and Brown*, 2005; *Rachold et al.*, 2003]. Therefore, a broad assessment of permafrost carbon dynamics needs to take into account that the release of permafrost-stored carbon is not only a near surface process involving shallow permafrost soil carbon pools in the active layer and thawing soils but also includes the transfer of carbon from deeper permafrost stores to the hydrosphere and atmosphere by disturbances such as thermokarst and erosion [*Schuur et al.*, 2008; *Grosse et al.*, 2011].

[30] Generally, OM stored in permafrost still represents a very poorly constrained pool in the global carbon cycle, which is only recently begun to be included in any current global carbon cycle model framework. However, recent attempts to inventory carbon pools in the Arctic and especially in near-surface soils and deeper sediments in permafrost regions have shown the potentially very large size of soil carbon stored in the permafrost region [*McGuire et al.*, 2009; *Tarnocai et al.*, 2009; *Zimov et al.*, 2009]. These studies also highlighted the existing uncertainties in current estimates and the need for more detailed assessments of such carbon pools and the character of OM, and a denser coverage with field data on shallow and deep carbon. For the peatland component of the permafrost soil carbon pool relative good estimates of carbon distribution with depth exist based on peatland inventories and thousands of peat cores from the circum Arctic [*Gorham*, 1991; *Smith et al.*, 2004; *Tarnocai et al.*, 2000; *Jones and Yu*, 2010]. For mineral soils in permafrost regions, however, such spatial and depth information is still very rare, though it has been shown that including deeper permafrost and soil strata into carbon inventories considerably increases the permafrost carbon pool [*Bockheim and Hinkel*, 2007; *Ping et al.*, 2008]. As many of these deeper carbon pools are nevertheless vulnerable to thaw and OM release due to a variety of well documented permafrost degradation processes, their characterization is an important task. Further attempts to tackle this data paucity for high-latitude systems are on the way for example by creating geospatial soil carbon databases including deeper deposits, such as currently in progress for Alaska [*Johnson and Harden*, 2009].

[31] For Siberia, a first-order estimate of organic carbon stored in the Ice Complex of the Yedoma Suite was attempted by *Zimov et al.* [2006a, 2006b], assuming general and homogeneous values for TOC content (2.6%), massive ice content (50%), bulk density ($1.65\ 10^3$ kg m^{-3}), thickness (25 m), and spatial distribution (1 million km^2) for this strata.

[32] The data presented in this paper, when coupled with direct measurements of bulk density from a subset of Yedoma Ice Complex sites [*Dutta et al.*, 2006] allow us to improve the first-order carbon inventory calculation by

increasing the number of percent C measurements and soil bulk density estimates by an order of magnitude. Interestingly, the percent C measurements shown here largely validate the early estimates of *Zimov et al.* [2006a, 2006b]. However, the bulk density estimates, calculated from the direct sediment ice content measurements, are lower by a factor of about 2, thus decreasing previous average permafrost C inventories by 25 to 50%. While the empirical bulk density conversion from ice content is based only on a small subset of Ice Complex samples (n = 13), the measured tight negative correlation (R^2 = 0.94) between ice content and frozen sediment bulk density (Figure 4), as well as the direct theoretical link between those two variables, increases our confidence in downwardly revising sediment bulk density values, and thus organic C inventory (kg C m^{-3}) for the Yedoma Ice. In addition, the new lower bulk density measurements presented here are consistent with bulk density measured across a range of Alaskan permafrost mineral soils (*E.A.S. Schuur*, unpublished data). Despite this refinement of the organic C inventory estimate, there still remain large organic C pools frozen at great depth in permafrost and this C pool remains vulnerable to climate change [*Schuur et al.*, 2008].

[33] When calculating the potential of future greenhouse gas release from decomposition of OM from degrading Ice Complex deposits or similar ice-rich permafrost, several current knowledge gaps should be taken into account. Variables that determine organic carbon content (weight per soil volume) are carbon concentration, ice content, the distribution of massive ice bodies, soil bulk density, and spatial extent and average depth of the particular permafrost units. Here, we have increased the number of carbon concentration and bulk density estimates (based on ice content) of late Quaternary Ice Complex deposits in Yedoma landscapes (about 500 samples) by roughly an order of magnitude whereas the remaining 3 variables still have large uncertainty that should be addressed by future studies.

[34] 1. Ice-rich permafrost contains roughly 50 to 80 vol % massive ice, which occurs as huge ice wedges and segregated ice, which distinctively lowers the total carbon pool on the landscape scale [*Schirrmeister et al.*, 2011b].

[35] 2. The spatial distribution of Ice Complex in Siberian Arctic lowlands is only approximately known [*Romanovskii*, 1993]. The distribution of similar deposits in Alaska and Canada is increasingly documented [*Kanevskiy et al.*, 2011].

[36] 3. The morphology of Siberian Arctic lowlands is dominated by Holocene thermokarst basins and only remnants of late Pleistocene Yedoma hills with Ice Complex deposits are preserved [e.g., *Grosse et al.*, 2007], so the average thickness and in particular the area of Ice Complex across the region is significantly reduced. Last, stratigraphical units within permafrost deposits reveal highly variable OM contents and qualities with depth (this study). This has considerable effects on both the total C inventory and the spatial structure (location) of the C inventory.

[37] In addition to these factors that control carbon pool size, the variation in OM quality with depth demonstrated in this study reflect past climate-driven factors that preceded C incorporation into permafrost, and will also control the release rate of this carbon with further thawing of permafrost. Therefore, specific biochemical analyses of OM to understand the lability of carbon in permafrost and its bioavailability for decomposition upon thawing are necessary in order to understand the potential rate of C release once thawed [*Dutta et al.*, 2006; *Schuur et al.*, 2009; *Zimov et al.*, 2006b].

[38] Ultimately, the vulnerability of the permafrost carbon pool to climate change [*Schuur et al.*, 2008] is connected to the vulnerability of permafrost to the direct effects of climate change [*Jorgenson et al.*, 2010] or resulting disturbances, such as thermokarst or wildfires [*Grosse et al.*, 2011]. Most recent analyses of permafrost temperature trends indicate that a continued warming occurred over the last decades in Siberia as well as in most other Arctic regions [*Romanovsky et al.*, 2010], pointing to profound changes in the future stability of at least parts of the current permafrost carbon pool and the potential thawing, decomposition and release of old carbon into the active carbon cycle by microbially generated greenhouse gas emissions and dissolved and particulate organic C transfer into the hydrosphere.

6. Conclusions

[39] We presented one of the first in-depth studies on the complexity of OM distribution for the upper permafrost zone up to 100 m depth in the northeastern Siberian Arctic, indicating that considerable variability of OM distribution between different stratigraphical units, between the same stratigraphical unit at different study sites, and even within stratigraphic units at the same site, are important factors that need to be taken into account in future inventories. Studies of paleoenvironmental properties and organic carbon biogeochemistry are important for better understanding of the origin, preservation, distribution, total inventory and vulnerability of OM in permafrost deposits. Both tools are necessary to determine the role of permafrost-stored organic carbon in the global carbon cycle.

[40] TOC contents at our study sites vary between 0.1 to 45.2 wt %, TIC contents between 0 to 7.2 wt %, C/N ratios between 0.03 to 38.4, and $\delta^{13}C$ values between −31.0 to −23.4‰. For individual strata, OM accumulation, preservation, and distribution are strongly linked to a broad variety of paleoenvironmental factors and specific surface and subsurface conditions before inclusion of OM into the permafrost.

[41] Based on our own data and scarcely existing literature data on stratigraphical differences and spatial variation of organic carbon sequestered in late Quaternary permafrost deposits, we believe that knowledge about the quantities and qualities of this potentially significant OM pool is still too limited for extrapolating to larger spatial scales. However, by combination of TOC and ice content measurements, and new bulk density estimates, this approach downwardly revises the overall carbon inventory. Further work on thickness and proportion of massive ice bodies and the distribution of permafrost strata will help to extrapolate to larger spatial scales. The enhancement of detailed regional permafrost spatial databases and regional organic carbon inventories, in combination with targeted field studies of deep soil organic carbon in permafrost regions, would be a

logical next step to alleviate these challenges [e.g., *Tarnocai et al.*, 2000; *Johnson and Harden*, 2009].

[42] **Acknowledgments.** We acknowledge support of this research by German Ministry of Science and Education (Russian-German science collaboration "Laptev Sea System") and the German Research Foundation (DFG, SCHI 975/1–2, KI 849). G. Grosse was partially supported by NASA NNX08AJ37G and NSF ARC-0732735. E. Schuur was partially supported by NSF grants 0747195, 0516326, and 0620579. We also thank the many Russian and German partners that were involved in more than 10 years of field research in the Siberian Arctic. Special thanks go to Ute Bastian and colleagues for the analytical work in the laboratories at the Alfred Wegener Institute, Department of Periglacial Research Unit in Potsdam.

References

Anderson, P. M., and A. V. Lozhkin (2001), The stage 3 interstadial complex (Karginskii/middle Wisconsinan interval) of Beringia: Variations in paleoenvironments and implications for paleoclimatic interpretations, *Quat. Sci. Rev.*, *20*, 93–125, doi:10.1016/S0277-3791(00)00129-3.

Andreev, A. A., et al. (2004), Late Saalian and Eemian palaeoenvironmental history of the Bol'shoy Lyakhovsky Island (Laptev Sea region, Arctic Siberia), *Boreas*, *33*, 319–348, doi:10.1080/03009480410001974.

Andreev, A. A., et al. (2009), Weichselian and Holocene palaeoenvironmental history of the Bol'shoy Lyakhovsky Island, New Siberian Archipelago, Arctic Siberia, *Boreas*, *38*, 72–110, doi:10.1111/j.1502-3885.2008.00039.x.

Andreev, A. A., L. Schirrmeister, P. E. Tarasov, A. Ganopolski, V. Brovkin, C. Siegert, S. Wetterich, and H.-W. Hubberten (2011), Vegetation and climate history in the Laptev Sea region (Arctic Siberia) during Late Quaternary inferred from pollen records, *Quat. Sci. Rev.*, doi:10.1016/j.quascirev.2010.12.026, in press.

Bockheim, J. G., and K. M. Hinkel (2007), The importance of "deep" organic carbon in permafrost-affected soils of Arctic Alaska, *Soil Sci. Soc. Am. J.*, *71*(6), 1889–1892, doi:10.2136/sssaj2007.0070N.

Carter, M. R., and E. G. Gregorich (Eds.) (2008), *Soil Sampling and Methods of Analysis*, 2nd ed., 1224 pp., Taylor and Francis, London.

Clark, I., and P. Fritz (1997), *Environmental Isotopes in Hydrology*, 328 pp., Lewis Publishers, New York.

Dutta, K., E. A. G. Schuur, J. C. Neff, and S. A. Zimov (2006), Potential carbon release from permafrost soils of northeastern Siberia, *Global Change Biol.*, *12*, 2336–2351, doi:10.1111/j.1365-2486.2006.01259.x.

Fraser, T. A., and C. R. Burn (1997), On the nature and origin of "muck" deposits in the Klondike area, Yukon Territory, *Can. J. Earth Sci.*, *34*, 1333–1344, doi:10.1139/e17-106.

French, H., and Y. Shur (2010), The principles of cryostratigraphy, *Earth Sci. Rev.*, *101*, 190–206, doi:10.1016/j.earscirev.2010.04.002.

Frey, K. E., and J. W. McClelland (2009), Impacts of permafrost degradation on arctic river biogeochemistry, *Hydrol. Processes*, *23*(1), 169–182, doi:10.1002/hyp.7196.

Giterman, R. E., A. V. Sher, and J. V. Matthew Jr. (1982), Comparison of the developments of tundra-steppe environment in west and east Beringia: Pollen and macrofossil evidence from key sections, in *Paleoecology of Beringia*, edited by D. M. Hopkins et al., pp. 43–73, Academic, New York.

Gorham, E. (1991), Northern peatlands: Role in the carbon cycle and probable responses to climatic warming, *Ecol. Appl.*, *1*, 182–195, doi:10.2307/1941811.

Grosse, G., L. Schirrmeister, C. Siegert, V. V. Kunitsky, E. A. Slagoda, A. A. Andreev, and A. Y. Dereviagyn (2007), Geological and geomorphological evolution of a sedimentary periglacial landscape in northeast Siberia during the Late Quaternary, *Geomorphology*, *86*, 25–51, doi:10.1016/j.geomorph.2006.08.005.

Grosse, G., et al. (2011), Vulnerability of high-latitude soil organic carbon in North America to disturbance, *J. Geophys. Res.*, *116*, G00K06, doi:10.1029/2010JG001507.

Gruber, N., P. Friedlingstein, C. B. Field, R. Valentini, M. Heimann, J. E. Richey, P. Romero-Lankao, E.-D. Schulze, and C.-T. A. Chen (2004), The vulnerability of the carbon cycle in the 21st century: An assessment of carbon-climate-human interactions, in *The Global Carbon Cycle: Integrating Humans, Climate, and the Natural World*, edited by C. B. Field and M. R. Raupach, pp. 45–76, Island Press, Washington, D. C.

Gundelwein, A., T. Müller-Lupp, M. Sommerkorn, E. T. K. Haupt, E.-M. Pfeiffer, and H. Wiechmann (2007), Carbon in tundra soils in the Lake Labaz region of arctic Siberia, *Eur. J. Soil Sci.*, *58*, 1164–1174, doi:10.1111/j.1365-2389.2007.00908.x.

Guthrie, R. D. (1990), *Frozen Fauna of the Mammoth Steppe*, 323 pp., Univ. of Chicago Press, Chicago, Ill.

Harden, J. W., C. C. Fuller, M. Wilmking, I. H. Meyers-Smith, S. E. Trumbore, and J. Bubier (2008), The fate of terrestrial carbon following permafrost degradation: Detecting changes over recent decades, in *Proceedings of the Ninth International Conference on Permafrost, June 29–July 3, 2008*, edited by D. L. Kane and K. M. Hinkel, pp. 649–654, Inst. of Northern Eng., Univ. of Alaska Fairbanks, Fairbanks.

Johnson, K., and J. Harden (2009), An Alaskan soil carbon database, *Eos Trans. AGU*, *90*(21), 184, doi:10.1029/2009EO210005.

Jones, M. C., and Z. Yu (2010), Rapid deglacial and early Holocene expansion of peatlands in Alaska, *Proc. Natl. Acad. Sci. U. S. A.*, *107*, 7347–7352, doi:10.1073/pnas.0911387107.

Jorgenson, M. T., and J. Brown (2005), Classification of the Alaskan Beaufort Sea Coast and estimation of carbon and sediment inputs from coastal erosion, *Geo-Mar. Lett.*, *25*(2–3), 69–80, doi:10.1007/s00367-004-0188-8.

Jorgenson, M. T., V. Romanovsky, J. Harden, Y. Shur, J. Donnell, E. A. G. Schuur, M. Kanevskiy, and S. Marchenko (2010), Resilience and vulnerability of permafrost to climate change, *Can. J. For. Res.*, *40*(7), 1219–1236, doi:10.1139/X10-060.

Kanevskiy, M., Y. Shur, D. Fortier, M. T. Jorgenson, and E. Stephani (2011), Cryostratigraphy of late Pleistocene syngenetic permafrost (yedoma) in northern Alaska, Itkillik River exposure, *Quat. Res.*, *75*, 584–596, doi:10.1016/j.yqres.2010.12.003.

Kaplina, T. N. (1981), History of frozen ground in northern Yakutia during the late Cenozoic, in *History of Permafrost Development in Eurasia* (in Russian), edited by V. V. Baulin and I. Dubikov, pp. 153–181, Nauka, Moscow.

Kienast, F., L. Schirrmeister, C. Siegert, and P. Tarasov (2005), Palaeobotanical evidence for warm summers in the East Siberian Arctic during the last cold stage, *Quat. Res.*, *63*(3), 283–300, doi:10.1016/j.yqres.2005.01.003.

Kienast, F., P. Tarasov, L. Schirrmeister, G. Grosse, and A. A. Andreev (2008), Continental climate in the East Siberian Arctic during the last interglacial: Implications from palaeobotanical records, *Global Planet. Change*, *60*(3–4), 535–562, doi:10.1016/j.gloplacha.2007.07.004.

Kienast, F., S. Wetterich, S. Kuzmina, L. Schirrmeister, A. Andreev, P. Tarasov, L. Nazarova, A. Kossler, L. Frolova, and V. V. Kunitsky (2011), Paleontological records indicate the occurrence of open woodlands in a dry inland climate at the present-day Arctic coast in western Beringia during the Last Interglacial, *Quat. Sci. Rev.*, doi:10.1016/j.quascirev.2010.11.024, in press.

McGuire, A. D., L. G. Anderson, T. R. Christensen, S. Dallimore, L. Guo, D. J. Hayes, M. Heimann, T. D. Lorenson, R. W. Macdonald, and N. Roulet (2009), Sensitivity of the carbon cycle in the Arctic to climate change, *Ecol. Monogr.*, *79*, 523–555, doi:10.1890/08-2025.1.

Meyers, P. A. (2003), Applications of organic geochemistry to paleolimnological reconstructions: A summary of examples from the Laurentian Great Lakes, *Org. Geochem.*, *34*(2), 261–289, doi:10.1016/S0146-6380(02)00168-7.

Péwé, T. L. (1975), *Quaternary Geology of Alaska*, *U.S. Geol. Surv. Prof. Pap.*, *835*, 145 pp.

Ping, C.-L., G. J. Michaelson, M. T. Jorgenson, J. M. Kimble, H. Epstein, V. E. Romanovsky, and D. A. Walker (2008), High stocks of soil organic carbon in the North American Arctic region, *Nat. Geosci.*, *1*(9), 615–619, doi:10.1038/ngeo284.

Rachold, V., H. Eicken, V. V. Gordeev, M. N. Grigoriev, H.-W. Hubberten, A. P. Lisitzin, V. P. Shevchenko, and L. Schirrmeister (2003), Modern terrigenous organic carbon input to the Arctic Ocean, in *Organic Carbon Cycle in the Arctic Ocean: Present and Past*, edited by R. Stein and R. W. Macdonald, pp. 33–55, Springer, Berlin.

Romanovskii, N. N. (1977), *Formations of Polygonal Ice-Wedge Structures* (in Russian), 218 pp., Sibirian Branch, Permafrost Inst., Acad. of Sci. of the USSR, Moscow.

Romanovskii, N. N. (1993), *Fundamentals of the Cryogenesis of the Lithosphere (Osnovy Kriogeneza Litosfery)* (in Russian), Univ. Press, Moscow.

Romanovsky, V. E., S. L. Smith, and H. H. Christiansen (2010), Permafrost thermal state in the polar Northern Hemisphere during the international polar year 2007–2009: A synthesis, *Permafrost Periglacial Processes*, *21*(2), 106–116, doi:10.1002/ppp.689.

Scheffer, F., and P. Schachtschabel (2002), *Lehrbuch der Bodenkunde* (in German), 593 pp., Spektrum, Heidelberg, Germany.

Schirrmeister, L., C. Siegert, T. Kuznetsova, S. Kuzmina, A. A. Andreev, F. Kienast, H. Meyer, and A. Bobrov (2002a), Paleoenvironmental and paleoclimatic records from permafrost deposits in the Arctic region of

northern Siberia, *Quat. Int.*, *89*, 97–118, doi:10.1016/S1040-6182(01)00083-0.

Schirrmeister, L., C. Siegert, V. V. Kunitzky, P. M. Grootes, and H. Erlenkeuser (2002b), Late Quaternary ice-rich permafrost sequences as a paleoenvironmental archive for the Laptev Sea Region in northern Siberia, *Int. J. Earth Sci.*, *91*, 154–167, doi:10.1007/s005310100205.

Schirrmeister, L., et al. (2003), Late Quaternary history of the accumulation plain north of the Chekanovsky Ridge (Lena Delta, Russia): A multidisciplinary approach, *Polar Geogr.*, *27*, 277–319, doi:10.1080/789610225.

Schirrmeister, L., et al. (2008), Periglacial landscape evolution and environmental changes of Arctic lowland areas for the last 60 000 years (western Laptev Sea coast, Cape Mamontov Klyk), *Polar Res.*, *27*(2), 249–272, doi:10.1111/j.1751-8369.2008.00067.x.

Schirrmeister, L., et al. (2010), The mystery of Bunge Land (New Siberian Archipelago): Implications for its formation based on palaeoenvironmental records, geomorphology, and remote sensing, *Quat. Sci. Rev.*, *29*, 3598–3614, doi:10.1016/j.quascirev.2009.11.017.

Schirrmeister, L., et al. (2011a), Late Quaternary paleoenvironmental records from the western Lena Delta, Arctic Siberia, *Palaeogeogr. Palaeoclimatol. Palaeoecol.*, *299*, 175–196, doi:10.1016/j.palaeo.2010.10.045.

Schirrmeister, L., V. Kunitsky, G. Grosse, S. Wetterich, H. Meyer, G. Schwamborn, O. Babiy, A. Derevyagin, and C. Siegert (2011b), Sedimentary characteristics and origin of the Late Pleistocene Ice Complex on north-east Siberian Arctic coastal lowlands and islands—A review, *Quat. Int.*, *241*, 3–25, doi:10.1016/j.quaint.2010.04.004.

Schleser, G. H. (1995), Parameters determining carbon isotope ratios in plants, in *Problems of Stable Isotopes in Tree-Rings, Lake Sediments and Peat Bogs as Climatic Evidence for the Holocene*, *Paleoclim. Res.*, vol. 15, edited by B. Frenzel, pp. 71–96, Akad. der Wiss. und der Literatur, Stuttgart, Germany.

Schuur, E. A. G., et al. (2008), Vulnerability of permafrost carbon to climate change: Implications for the global carbon cycle, *BioScience*, *58*(8), 701–714, doi:10.1641/B580807.

Schuur, E. A. G., J. Vogel, K. Crummer, H. Lee, J. Sickman, and T. Osterkamp (2009), The effect of permafrost thaw on old carbon release and net carbon exchange from tundra, *Nature*, *459*(7246), 556–559, doi:10.1038/nature08031.

Schwamborn, G., V. Rachold, and M. N. Grigoriev (2002), Late Quaternary sedimentation history of the Lena Delta, *Quat. Int.*, *89*, 119–134, doi:10.1016/S1040-6182(01)00084-2.

Sher, A. V., S. A. Kuzmina, T. V. Kuznetsova, and L. D. Sulerzhitsky (2005), New insights into the Weichselian environment and climate of the East Siberian Arctic, derived from fossil insects, plants, and mammals, *Quat. Sci. Rev.*, *24*, 533–569, doi:10.1016/j.quascirev.2004.09.007.

Smith, L. C., G. M. MacDonald, A. A. Velichko, D. W. Beilman, O. K. Borisova, K. E. Frey, K. V. Kremenetski, and Y. Sheng (2004), Siberian peatlands a net carbon sink and global methane source since the early Holocene, *Science*, *303*, 353–356, doi:10.1126/science.1090553.

Soloviev, P. A. (1959), *The Xryolithozone in the North Part of the Lena-Amga-Interfluve* (in Russian), 144 pp., Acad. of Sci. of the USSR, Moscow.

Strauss, J. (2010), Late Quaternary environmental dynamics at the Duvanny Yar key section, Lower Kolyma, East Siberia, diploma thesis, Inst. of Environ. and Earth Sci., Univ. of Potsdam, Potsdam, Germany.

Tarnocai, C., I. M. Kettles, and B. LeCelle (2000), Peatlands of Canada database, *Open File 3834*, Geol. Surv. of Can., Ottawa.

Tarnocai, C., J. G. Canadell, E. A. G. Schuur, P. Kuhry, G. Mazhitova, and S. A. Zimov (2009), Soil organic carbon pools in the northern circumpolar permafrost region, *Global Biogeochem. Cycles*, *23*, GB2023, doi:10.1029/2008GB003327.

Wagner, D., A. Gattinger, A. Embacher, E.-M. Pfeiffer, M. Schloter, and A. Lipski (2007), Methanogenic activity and biomass in Holocene permafrost deposits of the Lena Delta, Siberian Arctic and its implication for the global methane budget, *Global Change Biol.*, *13*, 1089–1099, doi:10.1111/j.1365-2486.2007.01331.x.

Walter, K. M., S. A. Zimov, J. P. Chanton, D. Verbyla, and F. S. Chapin (2006), Methane bubbling from Siberian thaw lakes as a positive feedback to climate warming, *Nature*, *443*(7107), 71–75, doi:10.1038/nature05040.

Walter, K. M., M. E. Edwards, G. Grosse, S. A. Zimov, and F. S. Chapin III (2007), Thermokarst lakes as a source of atmospheric CH4 during the Last Deglaciation, *Science*, *318*, 633–636, doi:10.1126/science.1142924.

Wetterich, S., L. Schirrmeister, and E. Pietrzeniuk (2005), Freshwater ostracodes in Quaternary permafrost deposits from the Siberian Arctic, *J. Paleolimnol.*, *34*, 363–376, doi:10.1007/s10933-005-5801-y.

Wetterich, S., S. Kuzmina, A. A. Andreev, F. Kienast, H. Meyer, L. Schirrmeister, T. Kuznetsova, and M. Sierralta (2008), Palaeoenvironmental dynamics inferred from late Quaternary permafrost deposits on Kurungnakh Island, Lena Delta, northeast Siberia, Russia, *Quat. Sci. Rev.*, *27*, 1523–1540, doi:10.1016/j.quascirev.2008.04.007.

Wetterich, S., L. Schirrmeister, A. A. Andreev, M. Pudenz, B. Plessen, H. Meyer, and V. V. Kunitsky (2009), Eemian and Late Glacial/Holocene palaeoenvironmental records from permafrost sequences at the Dmitry Laptev Strait (NE Siberia, Russia), *Palaeogeogr. Palaeoclimatol. Palaeoecol.*, *279*, 73–95, doi:10.1016/j.palaeo.2009.05.002.

White, R. E. (2006), *Principle and Practice in Soil Science*, 266 pp., Blackwell, Malden, Mass.

Winterfeld, M., L. Schirrmeister, M. N. Grigoriev, V. V. Kunitsky, A. Andreev, A. Murray, and P. P. Overduin (2011), Coastal permafrost landscape development since the Late Pleistocene in the western Laptev Sea, Siberia, *Boreas*, doi:10.1111/j.1502-3885.2011.00203.x, in press.

Yershov, E. D. (1989), *East Siberia and Far East* (in Russian), vol. 5, 515 pp., Nedra, Moscow.

Yershov, E. D. (1991), Geocryological map of Russia and neighbouring republics (in Russian), 1:2,500,000 scale, Moscow State Univ., Russian Ministry of Geology, Moscow. (English translation, P. J. Williams and M. T. Warren, Moscow State Univ., Moscow, 2003.)

Yurtsev, B. A. (2001), The Pleistocene tundra-steppe and the productivity paradox: The landscape approach, *Quat. Sci. Rev.*, *20*, 165–174, doi:10.1016/S0277-3791(00)00125-6.

Zimov, S. A., E. A. G. Schuur, and F. S. Chapin (2006a), Permafrost and the global carbon budget, *Science*, *312*, 1612–1613, doi:10.1126/science.1128908.

Zimov, S. A., S. P. Davydov, G. M. Zimova, A. I. Davydova, E. A. G. Schuur, K. Dutta, and F. S. Chapin III (2006b), Permafrost carbon: Stock and decomposability of a globally significant carbon pool, *Geophys. Res. Lett.*, *33*, L20502, doi:10.1029/2006GL027484.

Zimov, N. S., S. A. Zimov, A. E. Zimova, G. M. Zimova, V. I. Chuprynin, and F. S. Chapin III (2009), Carbon storage in permafrost and soils of the mammoth tundra-steppe biome: Role in the global carbon budget, *Geophys. Res. Lett.*, *36*, L02502, doi:10.1029/2008GL036332.

G. Grosse, Geophysical Institute, University of Alaska Fairbanks, 903 Koyukuk Dr., Fairbanks, AK 99775, USA.

H.-W. Hubberten, P. P. Overduin, L. Schirrmeister, J. Strauss, and S. Wetterich, Department of Periglacial Research, Alfred Wegener Institute for Polar and Marine Research, D-14473 Potsdam, Germany. (lutz.schirrmeister@awi.de)

E. A. G. Schuur, Department of Biology, University of Florida, 220 Bartram Hall, PO Box 118526, Gainesville, FL 32611, USA.